ARTICLE
Journal of Cellular Biochemistry 111:821–833 (2010)

Journal of Cellular Biochemistry

Characterization of Photodynamic Therapy Responses Elicited in A431 Cells Containing Intracellular Organelle-Localized Photofrin

Ya-Ju Hsieh,[1] Jau-Song Yu,[2*] and Ping-Chiang Lyu[1**]

[1] *Institute of Bioinformatics and Structural Biology, College of Life Science, National Tsing Hua University, Hsinchu, Taiwan, Republic of China*

[2] *Department of Cell and Molecular Biology, College of Medicine, Chang Gung University, Tao-Yuan, Taiwan, Republic of China*

ABSTRACT

Photodynamic therapy (PDT), a photochemotherapeutic regimen used to treat several diseases, including cancer, exerts its effects mainly through induction of cell death. Using human epidermoid carcinoma A431 cells as a model, we previously showed that distinct cell death types could be triggered by protocols that selectively delivered Photofrin (a clinically approved photosensitizer) to different subcellular sites (Hsieh et al. [2003] J Cell Physiol 194: 363–375). Here, the responses elicited by PDT in A431 cells containing intracellular organelle-localized Photofrin were further characterized. Two prominent cell phenotypes were observed under these conditions: one characterized by perinuclear vacuole (PV) formation 2–8 h after PDT followed by cell recovery or shrinkage within 48 h, and a second characterized by typical apoptotic features appearing within 4 h after PDT. DCFDA-sensitive reactive oxygen species formed proximal to PVs during the response to PDT, covering areas in which both endoplasmic reticulum (ER) and the Golgi complex were located. Biochemical analyses showed that Photofrin-PDT also induced JNK activation and altered the protein secretion profile. A more detailed examination of PV formation revealed that PVs were derived from the ER. The alteration of ER structure induced by PDT was similar to that triggered by thapsigargin, an ER Ca^{2+}-ATPase inhibitor that perturbs Ca^{2+} homeostasis, suggesting a role for Ca^{2+} in the formation of PVs. Microtubule dynamics did not significantly affect PV formation. This study demonstrates that cells in which intracellular organelles are selectively loaded with Photofrin mount a novel response to ER stress induced by PDT. J. Cell. Biochem. 111: 821–833, 2010.

KEY WORDS: PHOTODYNAMIC THERAPY; PHOTOFRIN; ENDOPLASMIC RETICULUM; VACUOLIZATION; CELL DEATH

Photodynamic therapy (PDT) was initially used in the management of non-malignant disease, such as actinic keratosis and Barrett's esophagus. In the last two decades, however, PDT has been approved by the U.S. Food and Drug Administration (FDA) and other health agencies in many countries for clinical management of various cancers, including those of the head and neck; the esophagus; and endobroncheal, lung, gastric, cervical, and papillary bladder cancers [Dougherty et al., 1998; Dolmans et al., 2003]. The therapy involves exposure of cells or tissues to a photosensitizing drug (a non-toxic dye) and harmless visible light in combination with oxygen to produce highly reactive oxygen species (ROS), which ultimately cause tumor destruction [Dolmans et al., 2003]. Several categories of photosensitizer have been used in PDT studies, including dyes such as Rose Bengal and methylene blue; drugs such as tetracyclines, chlorpromazine, 5-aminolaevulinic acid and Photofrin; and endogenous porphyrins [Halliwell and Gutteridge, 1989; Chan et al., 2000; Dolmans et al., 2003]. Photofrin, a hematoporphyrin derivative (HpD), is a first-generation PDT photosensitizer. Photofrin is the most widely used photosensitizer in clinical PDT and also the first drug approved by the FDA for

Abbreviations: DCFDA, 2′,7′-dichlorofluorescein diacetate; ER, endoplasmic reticulum; PARP, poly(ADP-ribose) polymerase; PDT, photodynamic therapy; PI, propidium iodide; PS, phosphatidylserine; PV, perinuclear vacuole; ROS, reactive oxygen species; SERCA, sarcoplasmic/endoplasmic reticulum calcium ATPase.

Additional Supporting Information may be found in the online version of this article.

Grant sponsor: Chang Gung University, Tao-Yuan, Taiwan, ROC; Grant number: CMRP1214; Grant sponsor: National Science Council of Taiwan, ROC; Grant number: NSC96-2320-B-182-031-MY3.

*Correspondence to: Dr. Jau-Song Yu, Department of Cell and Molecular Biology, College of Medicine, Chang Gung University, Taiwan, Republic of China. and Dr. Ping-Chiang Lyu, Institute of Bioinformatics and Structural Biology, College of Life Science, National Tsing Hua University, Hsinchu, Taiwan, Republic of China.
E-mail: yusong@mail.cgu.edu.tw; lslpc@life.nthu.edu.tw

Received 5 March 2010; Accepted 30 June 2010 • DOI 10.1002/jcb.22767 • © 2010 Wiley-Liss, Inc.
Published online 21 July 2010 in Wiley Online Library (wileyonlinelibrary.com).

cancer treatment. Although the mechanism remains unknown, Photofrin has a tendency to accumulate in highly proliferative tissues. The compound absorbs light up to ~640 nm; thus, irradiation of tissues with visible light excites the sensitizer. Upon absorption of a photon, the sensitizer is transformed from a ground state (singlet state) to an excited (triplet) state [Henderson and Dougherty, 1992]. In this triplet state, the sensitizer can induce two types of reactions. First, the sensitizer can react with directly biological substances, transferring a hydrogen atom to form radicals, which, in turn, interact with oxygen and generate oxygenated products. Alternatively, the triplet state of the sensitizer can transfer energy to oxygen in the ground state, generating singlet oxygen, a highly reactive form of oxygen that attacks many biological molecules, including lipids, proteins and nucleic acids, causing destruction of target cells [Girotti, 1990; Henderson and Dougherty, 1992; Woods et al., 2004; Sakharov et al., 2005]. Because PDT effects are oxygen-dependent, photosensitization is ineffective in anoxic areas of tissue, as previously demonstrated by an in vivo study [Gomer and Razum, 1984].

Studies from in vitro culture systems and in vivo animal models have shown that PDT has a direct effect on cancer cells, triggering multiple cell death modalities, including apoptosis, necrosis and autophagy [He et al., 1994; Oleinick et al., 2002; Marchal et al., 2005; Kessel et al., 2006]; these outcomes constitute the major therapeutic effects of PDT [Dolmans et al., 2003; Castano et al., 2006]. Biochemical analyses have revealed that Photofrin PDT induces lipid peroxidation and inactivation of plasma membrane enzymes [Gibson et al., 1988; Thomas and Girotti, 1989; Buettner et al., 1993], and also causes mitochondrial damage and inactivation of mitochondrial enzymes [Salet, 1986; Murant et al., 1987; Roberts et al., 1989]. It was initially reported that PDT killed cells via necrosis, but a 1991 report demonstrated for the first time that PDT could trigger apoptosis in mouse lymphoma cells [Agarwal et al., 1991]. Numerous subsequent studies have documented that PDT induces significantly different cell death phenotypes depending on the cell type, the photosensitizer used, the subcellular localization thereof, the total dose administered, the total light exposure dose, the light fluence rate, and the elapsed time between administration of the drug and light exposure. All these factors are interdependent [He et al., 1994; Dellinger, 1996; Noodt et al., 1996, 1999; Peng et al., 1996; Kessel et al., 1997; Luo and Kessel, 1997; Kessel and Luo, 1998; Hsieh et al., 2003].

The subcellular location of a photosensitizer is known to have a strong influence on the cell death response to photoactivation. Noodt et al. [1999] reported that different apoptotic pathways are induced from various intracellular sites by tetraphenylporphyrins and light. We and others have shown that necrosis predominates when Photofrin primarily targets the plasma membrane, whereas apoptosis is the principal response when Photofrin is internalized and photoirradiated [Dellinger, 1996; Hsieh et al., 2003]. Photofrin exhibits a dynamic distribution in human epidermoid carcinoma A431 cells; the compound is initially localized to the plasma membrane, but enters intracellular organelles [mainly the endoplasmic reticulum (ER)/Golgi apparatus, but also perinuclear sites] after prolonged incubation. PDT using plasma membrane-targeted Photofrin induces necrosis-like cell death in A431 cells, rather than causing typical apoptosis. PDT employing ER/Golgi-localized Photofrin results in varying death phenotypes depending on laser dose [Hsieh et al., 2003]. With a higher dose, A431 cells undergo apoptosis and apoptotic bodies appear. Lower-level laser treatment induces perinuclear vacuole (PV) formation. These data imply the existence of distinct signaling pathways that are differentially triggered when cells are subjected to different extents of PDT stress. However, the mechanisms responsible for these distinct cell phenotypes have not yet been clearly defined.

In the present study, we characterized the unique PV structures induced by PDT in A431 cells in which Photofrin is targeted mainly to intracellular organelles. We provide evidence that PVs are derived primarily from the ER, and show that PV formation is strongly linked to generation of ROS after PDT treatment. The possible involvement of microtubule assembly–disassembly and calcium homeostasis mechanisms in the regulation of PV formation was assessed using selective pharmacological inhibitors. Finally, we showed that PDT treatment modulated ERK and JNK activity and altered protein secretion.

MATERIALS AND METHODS

MATERIALS

Photofrin® was obtained from Quadra Logic Technologies (British Columbia, Canada). The ApoAlert Annexin V-FITC apoptosis kit and pEYFP-C3, pEYFP-ER, pEYFP-Golgi, pECFP-Peroxi, pECFP-Endo plasmids were from BD Biosciences Clontech (Palo Alto, CA). Anti-Mac-2 BP (I20) antibody was produced in rabbits as previously described [Wu et al., 2005]. Anti-p-JNK (G-7), anti-α-tubulin, anti-β-tubulin, anti-fibronectin and anti-p-ERK antibodies were from Santa Cruz Biotechnology (Santa Cruz, CA). Anti-PARP antibody was from Cell Signaling Technology (Beverly, MA). Thapsigargin, Taxol, nocodazole, L-histidine, D-mannitol and 2′,7′-dichlorofluorescein diacetate (DCFDA) were from Sigma (St. Louis, MO). The BCA protein assay reagent was from Pierce (Rockford, IL). FITC- and TRITC-conjugated secondary antibodies were from Jackson ImmunoResearch Laboratories (West Grove, PA).

CELL CULTURE AND PDT

Human epidermoid carcinoma A431 cells were cultured as previously described [Hsieh et al., 2003]. One day before experiments, cells were plated on 35-mm culture dishes. PDT was performed by incubating the cells in medium containing 28 μg/ml Photofrin (2.5 mg/ml stock solution in 5% dextrose) in the dark at 37°C for 3 h. After washing once with fresh medium, the cells were incubated in fresh medium for an additional 21 h and then irradiated with a 632.8 nm He–Ne laser (Coherent, Santa Clara, CA) at fluence rate of 15 mW, to yield total energies of 5 J/cm^2 (Type II PDT treatment) and 10 J/cm^2 (Type III PDT treatment). Both Types II and III treatment paradigms result in intracellular localization of Photofrin. To achieve a primarily plasma membrane localization of Photofrin, cells were incubated as described above for 3 h and then irradiated with 632.8 nm laser at 15 mW to 10 J/cm^2 (Type I PDT treatment). After incubating at 37°C in a humidified CO_2 incubator for the indicated times, the cells were washed twice with ice-cold PBS and lysed in 80 μl of lysis buffer (20 mM Tris–HCl pH 7.4, 1 mM EDTA, 1 mM EGTA, 1% Triton X-100, 1 mM benzamidine, 1 mM phenyl-

methylsulfonyl fluoride, 50 mM sodium fluoride, 20 mM sodium pyrophosphate, 1 mM sodium orthovanadate) on ice for 10 min. The cell lysates were sonicated on ice for 3×10 s followed by centrifugation at 15,000*g* for 20 min at 4°C. The resulting supernatants were used as the cell extracts.

COLLECTION OF PROTEINS SECRETED BY A431 CELLS

A431 cells were grown to confluence in 35-mm culture dishes. After PDT treatment, medium was replaced with serum-free medium and cells were incubated for 24 or 48 h. The conditioned media were harvested, centrifuged to eliminate intact cells, and concentrated on Amicon Ultra-15 centrifugal concentrators (molecular weight cutoff, 5 kDa; Millipore, Billerica, MA) by centrifuging three times at 3,700*g* for 40 min. The protein concentration in concentrated samples was determined using the BCA protein assay reagent.

CELL VIABILITY ASSAY

Cell viability was determined by the trypan blue dye exclusion assay.

IMMUNOBLOT

Immunoblotting was carried out essentially as described previously [Hsieh et al., 2003]. Briefly, proteins were resolved by SDS–PAGE, transferred to a PVDF membrane and then probed with the indicated antibodies.

DETECTION OF APOPTOSIS

Phosphatidylserine (PS) externalization and propidium iodide (PI)-staining of nuclei were detected using the ApoAlert Annexin V-FITC apoptosis kit, as previously described [Hsieh et al., 2003]. Briefly, A431 cells grown on glass slide were treated with PDT. After washing with binding buffer, cells were incubated with 5 μl of Annexin V-FITC and 10 μl of PI in the dark at room temperature for 10 min, followed by fixation with 2% formaldehyde. Slides were then analyzed under a fluorescence microscope (Axioplan II).

DETECTION OF INTRACELLULAR ROS

ROS formation in cells was detected using the fluorescent probe DCFDA. A431 cells grown on coverslip were incubated in culture medium containing 28 μg/ml Photofrin in the dark at 37°C for 3 h. After washing once with fresh medium, the cells were incubated in fresh medium for an additional 21 h. One hour prior to the end of this incubation, DCFDA was added to the medium to a final concentration of 100 μM. The cells were then laser-irradiated, incubated in a CO_2 incubator for 4 h, and observed under a fluorescence microscope (Axioplan II).

IMMUNOSTAINING

Immunostaining was performed essentially as previously described [Hsu et al., 2010]. A431 cells were grown on coverslips and then subjected to type II PDT treatment. After treatment, cells were fixed with 3.7% formaldehyde at room temperature for 15 min, permeabilized with 0.2% Triton X-100 for 10 min, blocked with 5 mg/ml BSA for 1 h and stained with primary antibody diluted 1:200 in blocking solution for 3 h. FITC- or TRITC-conjugated secondary antibodies diluted 1:200 in blocking solution were then added and incubated for 1 h. After the wash steps, the cells on coverslips were mounted and observed under a fluorescence microscope (Axioplan II).

SELECTION OF A431 CELL LINES STABLY EXPRESSING ORGANELLE TRACKERS

A431 cells were separately transfected with the control plasmid pEYFP-C3 or various organelle tracker plasmids (pEYFP-ER, pEYFP-Golgi, pECFP-Peroxi and pECFP-Endo) using Lipofectamine™ 2000 (Invitrogen, Carlsbad, CA), according to the provided protocol. Cells that stably expressed fluorescent proteins were selected by culturing with 800 μg/ml G418, and then were maintained in regular culture medium containing 400 μg/ml G418.

LIVE-CELL IMAGING

A431 cells stably expressing EYFP-ER tracker were grown on coverslips and subjected to type II PDT treatment. The coverslips were then placed into the POC-R chamber and observed under a fluorescence microscope with a time-lapse system (Axiovert 200M microscope, Carl Zeiss AxioCam HR CCD camera, CTI controller 3700, and Tempcontrol 37-2 digital, Zeiss, Germany). Images were collected every 2 min by irradiating cells for 1 s with fluorescence light and/or 0.1 s with halogen light.

RESULTS

PHENOTYPIC CHARACTERISTICS OF A431 CELLS FOLLOWING EXPOSURE TO DIFFERENT PHOTOFRIN-PDT REGIMENS

We previously reported a dynamic distribution of Photofrin in A431 cells, showing that Photofrin was distributed first to plasma membranes, moving after prolonged incubation to intracellular compartments, mainly the Golgi complex and other intracellular organelles [Hsieh et al., 2003]. Although we earlier characterized, in detail, the effects of Photofrin-PDT on A431 cells under conditions in which the plasma membrane is the main target, the PDT-elicited responses of A431 cells containing intracellular organelle-localized Photofrin have not yet been defined. As variations in Photofrin distribution might result in different effects after PDT treatment, we re-examined the responses of PDT-treated A431 cells using various incubation protocols and different laser doses, tentatively designated types I, II and III treatments (see legend to Fig. 1 for details of each condition), in the presence or absence of Photofrin. In agreement with our previous study [Hsieh et al., 2003], the cell death phenotype was primarily necrotic when Photofrin was distributed mainly in/on the plasma membrane (Fig. 1A; type I treatment). When cells were transiently exposed to Photofrin and next incubated for a longer period of time, allowing Photofrin to diffuse into intracellular organelles, PDT treatment with 10 J of laser energy (type III treatment) induced cell shrinkage and membrane blebbing, resembling apoptosis. In contrast, PDT treatment with lower laser energy (5 J, type II treatment) after the same Photofrin incubation period triggered the formation of PVs inside cells (Fig. 1A), indicating that irradiation of Photofrin-loaded intracellular organelles with different laser doses resulted in distinct cellular responses. To characterize the cell response phenotypes, we determined whether typical indicators of apoptosis, including PS externalization and DNA condensation/fragmentation, could be detected in A431 cells

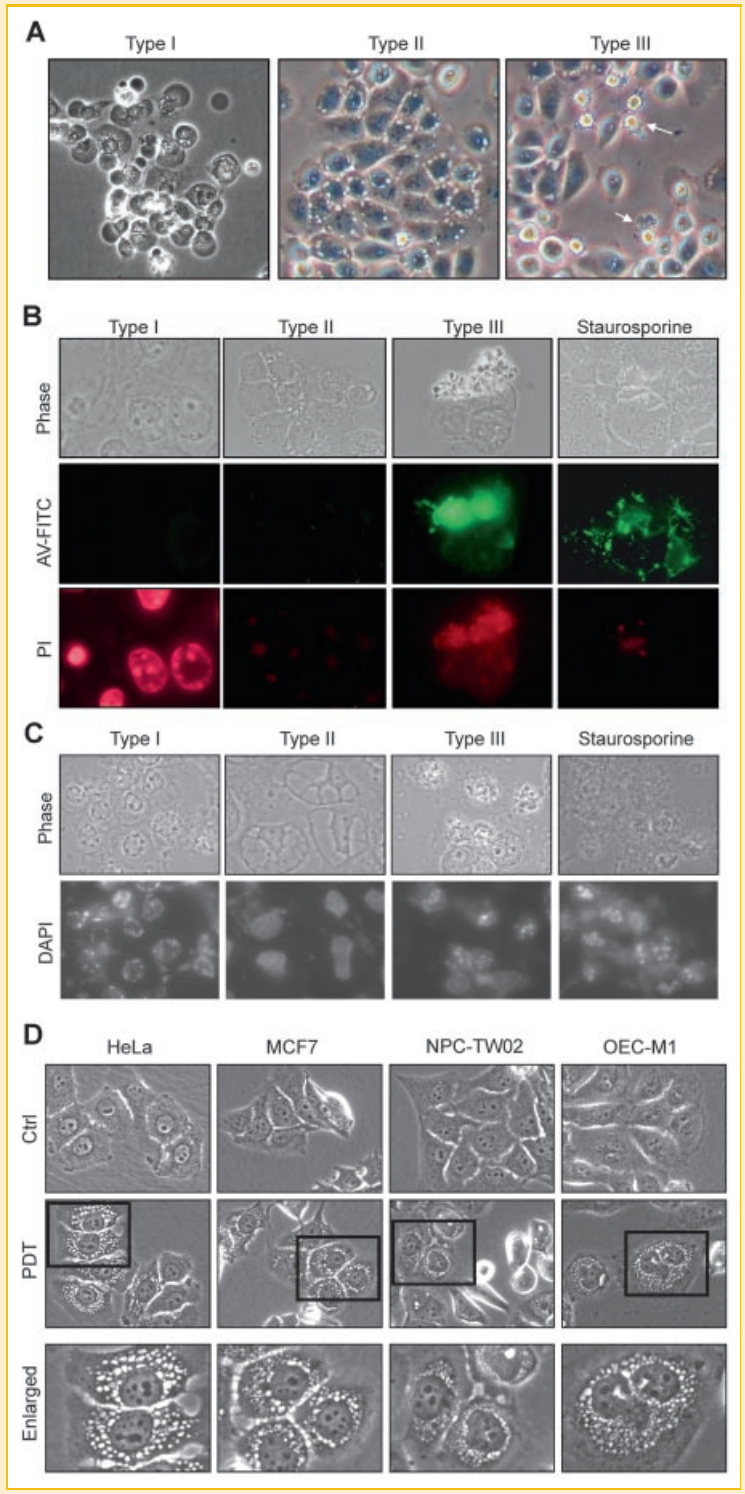

Fig. 1. Distinct cell death types and morphological changes induced in A431 cells by different Photofrin-PDT regimens. A: A431 cells grown on 35-mm dishes were exposed to three different treatment regimens: (1) *Type I treatment*: Incubation with Photofrin (28 μg/ml) for 3 h, two washes in fresh medium, followed by irradiation with a 632.8 nm laser at 15 mW output to a total of 10 J/cm^2. *Type II treatment*: Incubation with Photofrin (28 μg/ml) for 3 h, two washes in fresh medium, incubation in fresh medium without Photofrin for 21 h, followed by laser irradiation to 5 J/cm^2; *Type III treatment*: The same as type II treatment except cells were irradiated to a total of 10 J/cm^2. Cell morphology was observed 4 h after PDT treatment. B: A431 cells grown on glass slides were treated with different PDT protocols as described in (A) above and next incubated at 37°C for 4 h. Thereafter, cells were double-stained with annexin V (AV-FITC) and propidium iodide (PI), and observed under a fluorescence microscope. Cells treated with staurosporine (1 μM for 6 h) were used as a positive control. C: Cells treated as described in (B) were stained with DAPI to detect DNA fragmentation. D: HeLa (cervical carcinoma), MCF7 (breast cancer), NPC-TW02 (nasopharyngeal carcinoma), and OECM1 (oral cancer) cells were left untreated (Ctrl) or treated with type II PDT (PDT) and observed under a microscope 5 h after treatment. *Lower panel*: Enlargement of boxed areas in the middle panel. [Color figure can be viewed in the online issue, which is available at wileyonlinelibrary.com.]

after different treatments (Fig. 1B,C). The results showed that PS externalization occurred only upon type III treatment, whereas DNA condensation was observed following both types I and III, but not type II treatment. These observations indicate that type II PDT treatment can damage intracellular organelles and lead to PV formation in A431 cells. To determine whether type II PDT treatment-induced PV formation is a cell type-specific event or is common to different cell types, we performed similar experiments using four additional cell lines: HeLa (cervical carcinoma), MCF7 (breast cancer), NPC-TW02 (nasopharyngeal carcinoma) and OECM1 (oral cancer). We found that PVs formed in all cell lines tested (Fig. 1D), suggesting that PV formation is a common response of cancer cell lines to type II PDT treatment. Because this particular phenotypic change in response to Photofrin-PDT has not been previously reported, we characterized the change in more detail, as described below.

TYPE II PDT TREATMENT REDUCES VIABILITY AND IMPAIRS PROTEIN SECRETION BY A431 CELLS

We found that PV formation in A431 cells could be detected approximately 2 h after type II PDT treatment, at which point some treated cells had begun to detach from the surface of the culture dish, suggesting a loss of cell viability. Using the trypan blue exclusion assay, we indeed observed a reduction (~30%) in the viability of A431 cells after type II PDT treatment (Fig. 2A). Laser irradiation or Photofrin treatment alone had little effect on viability. The loss of viability after type II PDT treatment was accompanied by increased cleavage of poly-(ADP-ribose) polymerase (PARP), that was

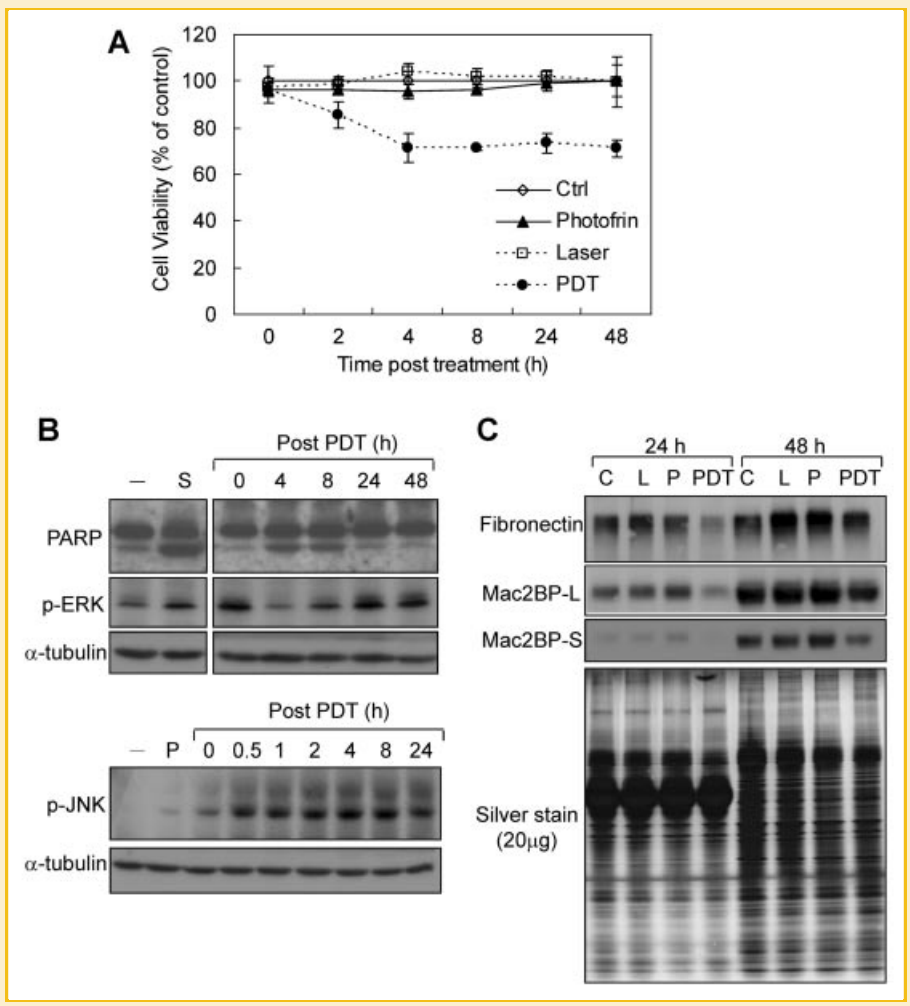

Fig. 2. Effects of type II PDT treatment on the viability, MAPK activity, and protein secretion of A431 cells. A: A431 cells were left untreated (Ctrl), treated with Photofrin or laser alone, or exposed to type II PDT treatment. The cells were then incubated at 37°C, and assayed after various time intervals for viability using a trypan blue dye exclusion assay. The results were obtained from three independent experiments and expressed as means ± SD. B: Proteins (60 μg aliquots) from cell extracts prepared at different times after PDT treatment were resolved by SDS–PAGE and immunoblotted with antibodies against PARP, p-ERK and p-JNK. The immunoblot signal of α-tubulin shown in the lower panel was used as the internal control. S: extracts from cells treated with 1 μM staurosporine (positive control); P: Photofrin (28 μg/ml) treatment without laser exposure. C: Immunoblotting to detect fibronectin and Mac-2 BP secreted from A431 cells with or without Photofrin-PDT treatment. Conditioned media from A431 cells were collected 24 and 48 h after type II PDT treatment; 60 μg aliquots of medium proteins were resolved by SDS–PAGE on 8–15% (w/v) gradient gels and immunoblotted with antibodies against fibronectin and Mac-2 BP. Secreted proteins (20 μg) collected from each experimental condition were resolved by SDS–PAGE and silver stained to serve as loading control. C: untreated control cells; L: cells exposed to laser light only; P: cells treated with Photofrin only; Mac-2 BP (L) and (S): longer and shorter X-ray film exposure times, respectively.

detectable 4 h after treatment. However, the level of the 85-kDa PARP fragment generated by PDT was much less than detected in cells treated with staurosporine, a known protein kinase C (PKC) inhibitor and a potent inducer of apoptosis (Fig. 2B). Interestingly, after 24- and 48-h incubation, the extent of PARP cleavage in PDT-treated cells decreased to a level comparable to that of untreated cells, suggesting that dead cells may have been eliminated and damaged live cells might have recovered. c-Jun N-terminal kinase (JNK), a kinase commonly activated under various stress conditions, including type I PDT treatment [Hsieh et al., 2003], was also activated within 30 min after treatment and sustained the activated state for at least 8 h (Fig. 2B). Extracellular signal-regulated kinase (ERK) activity followed a different pattern; ERK activity increased immediately after PDT, was down-regulated at 4–8 h, and returned to original post-treatment activation levels within 24 h (Fig. 2B).

To investigate whether type II PDT treatment affected cellular protein secretion, we harvested 24- and 48-h conditioned media from type II PDT-treated and untreated A431 cells, and measured the levels of fibronectin and Mac-2 binding protein (Mac-2 BP), two proteins that are well-known to be secreted [Wu et al., 2005], by immunoblotting. As shown in Figure 2C, both fibronectin and Mac-2 BP levels in conditioned media were significantly decreased in PDT-treated cells compared with untreated cells and cells exposed to laser or Photofrin alone. This suggests that type II PDT treatment has a profound effect on the protein secretion pathway, probably because of damage suffered by intracellular organelles, such as the Golgi apparatus and ER.

LOCALIZATION OF INTRACELLULAR ROS FORMED IN LIVE CELLS AFTER PDT

ROS are known to be the active molecules generated by PDT treatment, and can attack nearby proteins, DNA, lipids, and biomolecules. Because of their high reactivity and short half-life, ROS generated by PDT affect only cellular components close to the area of ROS production (i.e., adjacent to the photosensitizer) [Moan and Berg, 1991]. The half-life of singlet oxygen in biological systems is $<0.04\,\mu s$, and the radius of action of singlet oxygen is $<0.02\,\mu m$ [Moan and Berg, 1991]. To examine the location(s) of ROS generated in PDT-treated A431 cells with organelle-localized Photofrin, we further incubated Photofrin-preloaded cells for an appropriate time with DCFDA, a cell-permeable ROS-sensitive dye frequently used to monitor intracellular oxidative stress [LeBel et al., 1992], and next irradiated cells with a laser. In untreated cells and cells treated with Photofrin or laser alone, only background or very low levels of oxidized DCFDA were detected (Fig. 3A). Four hours after irradiation, fluorescence microscopy revealed a drastic change in cell morphology, including the formation of PVs, in cells in which Photofrin was targeted to intracellular organelles (Fig. 3B). Notably, DCFDA fluorescence was present mainly around PVs, a distribution that coincided well with the location of Photofrin. These findings suggest that PDT-induced PVs could result from organellar damage caused by newly generated adjacent ROS. Moreover, cells pretreated with L-histidine, a commonly used singlet oxygen scavenger, showed delayed PV formation during type II PDT treatment and the percentage of cells harboring PVs 2 h post-PDT was significantly reduced (Supplemental Fig. S1). In contrast, mannitol, a known hydroxyl radical scavenger that quenches the hydroxyl radical rather specifically, because of a low rate constant for reaction with singlet oxygen [Halliwell and Gutteridge, 1989], had no such effect on PV formation. These observations implicate singlet oxygen as the major type of ROS generated by Photofrin-PDT and the likely candidate for induction of vacuole formation in A431 cells.

CHARACTERIZATION OF PVs

First, we considered the possibility that PVs might be derived from digestive organelles, such as peroxysomes, lysosomes or autophagosomes. To test this hypothesis, we stained PDT-treated cells with monodansylcadaverine (MDC) to detect autophagy, or with acridine orange to display acidic vesicles. The PVs were not stained by either dye (data not shown), suggesting that they are likely not derived from autophagosomes or lysosome-related structures. To more directly explore the origin of PVs, we generated stably transfected A431 cell lines separately expressing various organelle trackers tagged with different fluorescent proteins, including pEYFP-Golgi, pEYFP-ER, pECFP-Peroxi, and pECFP-Endo; the pEGFP-C3 plasmid was used as a control. The transfected strains expressed the fluorescent organelle trackers at the expected subcellular sites (Fig. 4A). After type II PDT treatment, most, if not all, EYFP-ER tracker was concentrated in discrete, lucent globular structures that closely matched the PVs observed under phase-contrast microscopy. In contrast, other organelle trackers were barely incorporated into PVs (Fig. 4B,C). In control (untreated) cells, the EYFP-ER protein showed a reticular distribution in the cytoplasm. These findings suggest that the PVs formed in response to type II PDT treatment are derived from the ER by dilation of the ER cisternae.

We next recorded live images of A431 cells undergoing type II PDT treatment. Time-lapse videography revealed that the vacuoles were initially few and small, and were predominantly localized in the perinuclear region (Fig. 5; also see Supplemental Video 1). Under conditions in which microscopic recordings were collected under frequent halogen light irradiation (0.1 s irradiation every 2 min), vesicles formed within 1 h after PDT treatment, significantly shorter than the time ($\sim$2 h) required for type II PDT treatment to initially induce vacuole formation in cells placed in a CO_2 incubator. Thereafter, small vacuoles continuously increased in number and apparently merged to form larger vacuoles, which eventually occupied the cytoplasmic space. Interestingly, assessments made 4 h after PDT treatment showed that cells in which vacuoles formed could undergo one of two totally different fates: some cells died with cell shrinkage and membrane blebbing (Fig. 5, arrows), whereas others recovered from ER vacuolization and survived (Fig. 5, arrowheads). We also monitored vacuole formation at different time points by fluorescence microscopy using A431 cells stably expressing the EYFP-ER tracker (Supplemental Fig. S2). We observed that small vacuoles formed very rapidly (within 10 min) after PDT treatment, probably because the cells absorbed more energy from fluorescent light (100 W) than from laser irradiation (15 mW). Observations of the movement and fusion of vacuoles under continuous exposure to fluorescent light showed that most cells died within 3 h (data not shown). Collectively, these live-cell imaging

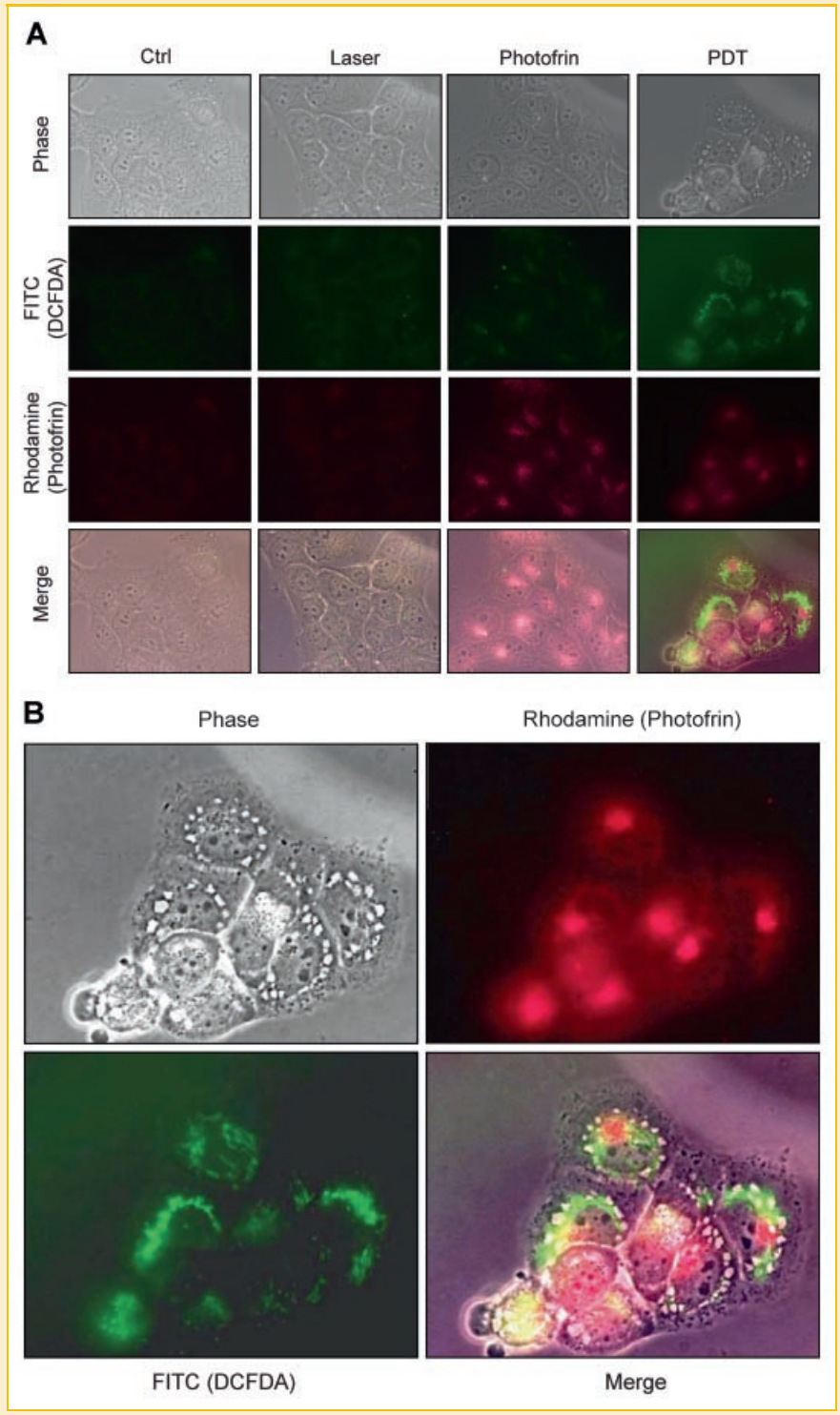

Fig. 3. ROS formation in the vicinity of PVs induced in A431 cells by type II PDT treatment. A: A431 cells grown on glass slides were left untreated (Ctrl), treated with Photofrin or laser alone, or exposed to type II PDT treatment. DCFDA (100 μM) was added to the culture medium 1 h before laser irradiation. Living cells were observed under a fluorescence microscope 4 h after PDT treatment. Phase: cell morphology; Rhodamine: Photofrin location; FITC: DCFDA fluorescence; Merge: phase merged with FITC and rhodamine images. B: Enlarged images of PDT-treated cells in (A).

data not only demonstrate the dynamic nature of ER vacuole formation after type II PDT treatment, but also demonstrate the capacity of cells to recover from this form of PDT-triggered ER damage.

PERTURBATION OF MICROTUBULE DYNAMICS HAS LITTLE EFFECT ON PV FORMATION IN PDT-TREATED CELLS

Our data indicate that PVs are derived mainly from the ER. Because microtubules and some microtubule-associated proteins are

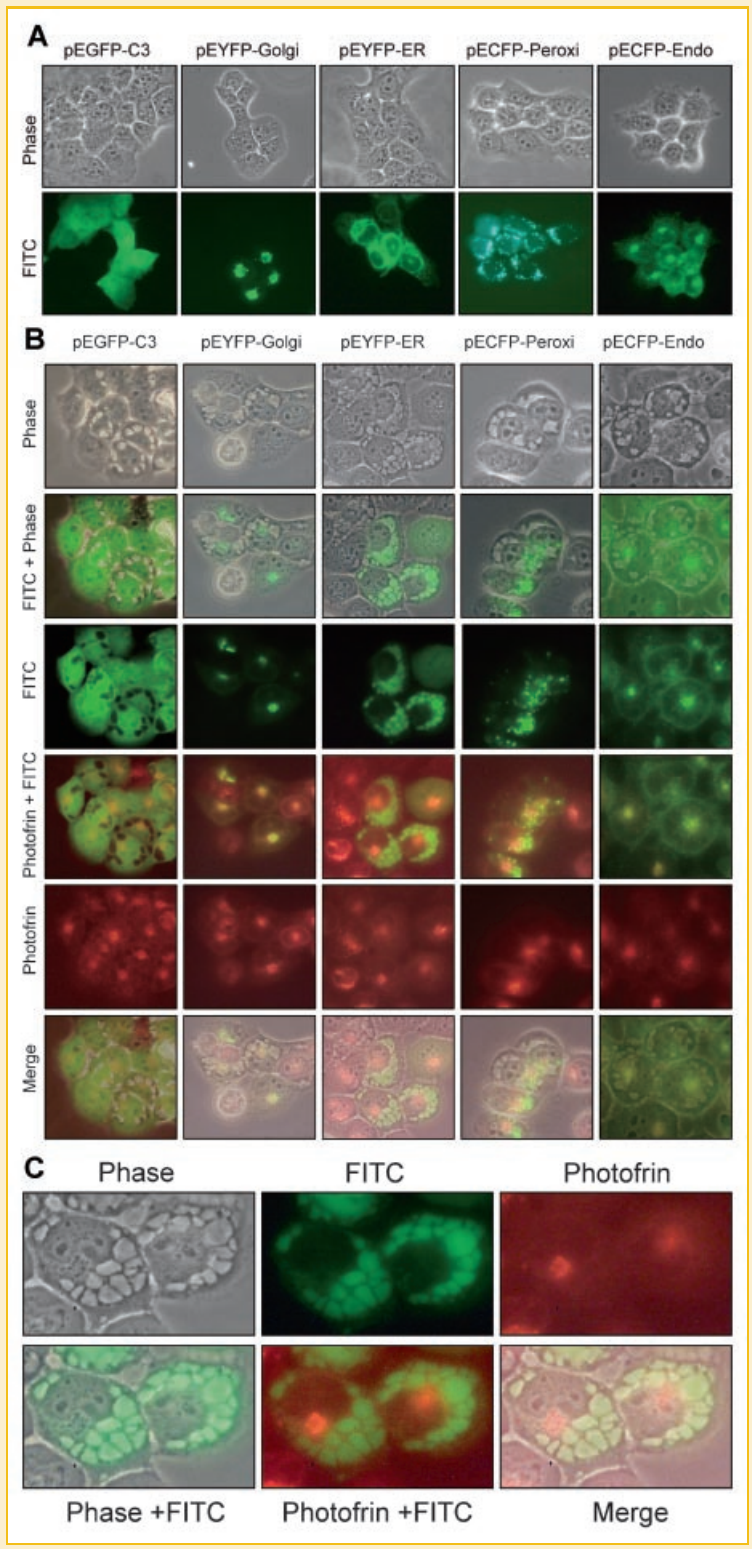

Fig. 4. Identification of the origin of PVs formed in PDT-treated cells using organelle trackers. A: A431 cells were transfected with various plasmids expressing specific fluorescent proteins tagged with different organelle trackers. Cells were exposed to G418 selection for 2 weeks and then observed under a fluorescence microscope. B: A431 cells stably expressing various organelle trackers were subjected to type II PDT treatment. Four hours after treatment, cells were observed under a fluorescence microscope. The locations of Photofrin (Zeiss Rho 15 filter) and organelle trackers (Zeiss FITC 10 filter) are shown. Images detecting PVs (phase), organelle trackers (FITC), and Photofrin were separately merged for comparative purposes. FITC + Phase: phase-contrast image merged with organelle tracker image (FITC); Photofrin + FITC: Photofrin image merged with organelle tracker image (FITC); Merge: phase-contrast image merged with images from organelle trackers (FITC) and Photofrin. C: Enlarged and cropped images from pEYFP-ER in (B).

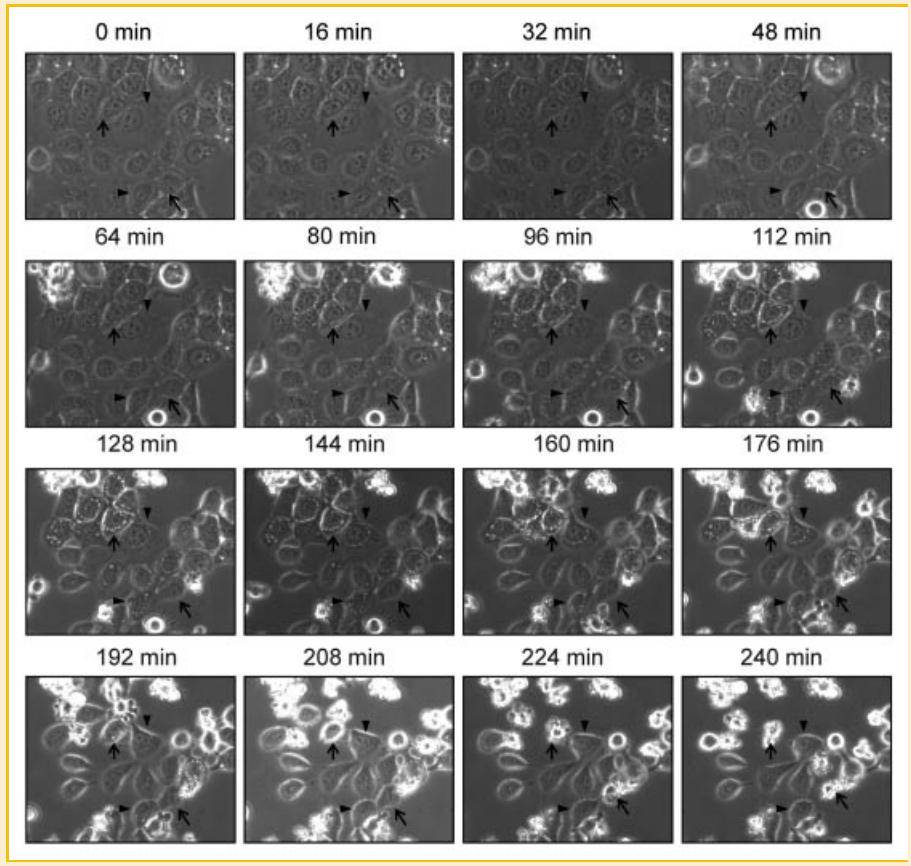

Fig. 5. Time-lapse observations of vesicle formation in A431 cells treated with type II PDT. A431 cells were subjected to type II PDT treatment, and next placed in a time-lapse system (Axiovert 200 M microscope, Carl Zeiss AxioCam HR CCD camera, CTI controller 3700, and Tempcontrol 37-2 digital system). Cells were observed under halogen light and images taken at 2-min intervals. Photographs taken at 16-min intervals. Arrows indicate cells that ultimately died after type II PDT treatment; arrowheads denote cells that recovered from ER vacuolization and survived.

essential for ER formation and structural maintenance [Du et al., 2004; Vedrenne and Hauri, 2006], we speculated that type II PDT treatment might cause alterations in the ER, by damaging microtubules. To test this possibility, we treated A431 cells with nocodazole (to destabilize microtubules) or Taxol (to stabilize microtubules) prior to PDT treatment, and next observed the effects of these agents on PDT-induced PV formation. As shown in Figure 6A–C, neither agent alone elicited PV formation. Moreover, neither microtubule destabilization with nocodazole nor microtubule stabilization with taxol significantly affected PV formation in PDT-treated cells (Fig. 6D–F).

THAPSIGARGIN, A SELECTIVE INHIBITOR OF SARCOPLASMIC/ENDOPLASMIC RETICULUM CALCIUM ATPASE (SERCA), ALSO INDUCES PV FORMATION IN A431 CELLS

The ER is a major calcium reservoir that is important for storing and regulating the level of intracellular calcium. This ER function is controlled principally by the sarcoplasmic/ER calcium ATPase (SERCA), a membrane protein that constantly pumps cellular calcium ions into the ER. Because our data implicate the ER as a major target of the effects of type II PDT treatment, we tested whether the PDT-induced ER response could be attributable to dysfunction of SERCA. To explore this hypothesis, we treated A431 cells stably expressing the EYFP-ER tracker with thapsigargin, a selective SERCA inhibitor that prevents calcium uptake by the ER and thus causes depletion of ER calcium stores [Denmeade and Isaacs, 2005]. A microscopic examination showed that cells treated with higher concentrations of thapsigargin contained many ER-derived vacuoles around the nucleus (Fig. 7), a phenotype similar to that of PDT-treated cells. This observation strongly suggests that SERCA may be a primary target affected by type II PDT treatment.

DISCUSSION

A number of biochemical studies have established that PDT using different sensitizers triggers multiple cell death modalities, including apoptosis, necrosis, and autophagy [He et al., 1994; Oleinick et al., 2002; Marchal et al., 2005; Kessel et al., 2006]. Moreover, it has long been known that the apoptosis pathway induced by PDT is heavily dependent on the subcellular distribution of the photosensitizer. Four different mechanisms of apoptosis have been reported, mediated by (1) the death receptor (the extrinsic pathway), (2) mitochondria (the intrinsic pathway), (3) ER stress and (4) a

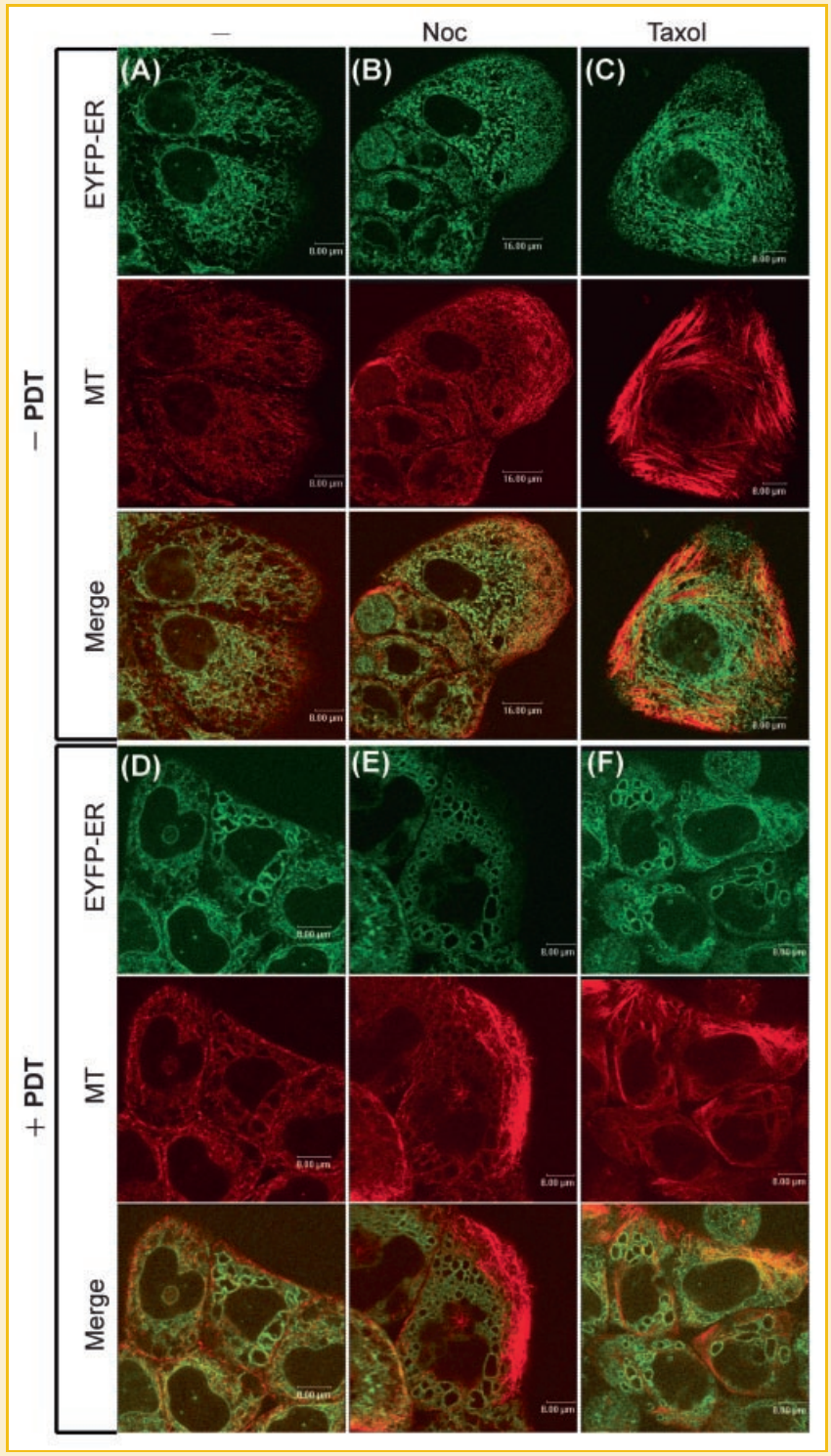

Fig. 6. Effects of nocodazole and Taxol on PDT-triggered ER vacuolization in A431 cells. A431 cells stably expressing EYFP-ER were left untreated (A–C) or were treated with the type II PDT protocol (D–F). During treatments, 1 μM taxol (C, F) or 1 μg/ml nocodazole (Noc) (B, E) was added to the culture medium 1 h before laser irradiation. Four hours after PDT treatment, cells were incubated with an anti-β-tubulin antibody to immunostain microtubules (MT) and were then observed under a fluorescence microscope. [Color figure can be viewed in the online issue, which is available at wileyonlinelibrary.com.]

caspase-independent process [Buytaert et al., 2007]. Intrinsic apoptosis can be initiated by signals originating from or converging on intracellular organelles, such as mitochondria, lysosomes or the ER [Danial and Korsmeyer, 2004].

The present study shows that the cell death induced by type II PDT treatment is neither autophagy nor necrosis, and provides several new insights into PDT-induced cell death/responses. First, we report that under conditions in which Photofrin is localized to intracellular

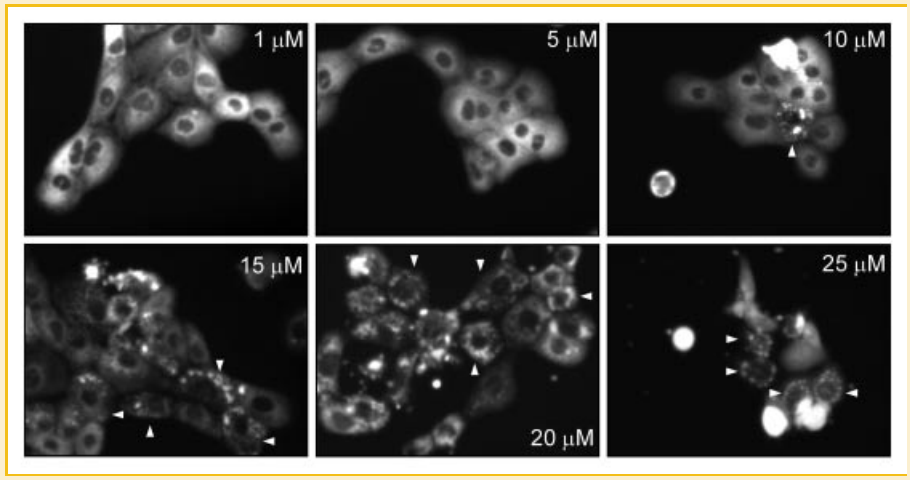

Fig. 7. Thapsigargin induces PV formation in A431 cells. A431 cells stably expressing EYFP-ER were treated with different concentrations (1, 5, 10, 15, 20 or 25 μM) of thapsigargin for 6 h. Alterations of the ER structure were observed under a fluorescence microscope. Arrows indicate cells showing PV formation.

organelles, the dose of laser irradiation is a determinant of cell fate. At higher laser doses, apoptosis represents the major type of cell death; at lower doses, cytoplasmic vacuolization occurs and may lead to either cell death or recovery. Second, we establish that the vacuoles induced by type II PDT treatment arise from dilated ER cisternae. Third, we show that ER vacuolization is accompanied by perturbation of protein secretion. Fourth, we demonstrate a very close correlation between ER vacuolization and ROS generation. Finally, we show that PDT-induced vacuolization can be mimicked using the selective SERCA inhibitor thapsigargin, suggesting that ER vacuolization could be an indication of Ca^{2+} imbalance, and implying that SERCA function might be compromised by type II PDT treatment.

Recent studies have suggested that the ER may act as a critical control point in several apoptotic pathways activated by stimuli that cause Ca^{2+} overload or perturb Ca^{2+} homeostasis [Demaurex and Distelhorst, 2003; Orrenius et al., 2003]. It has been reported that PDT treatment using hypericin or verteporfin as the photosensitizer leads to rapid disappearance of SERCA2, with subsequent depletion of ER Ca^{2+} and increased cytoplasmic Ca^{2+} levels [Granville et al., 2001; Buytaert et al., 2006], although any possible connection between intracellular Ca^{2+} levels and PDT-induced apoptosis has not yet been clearly defined.

A literature survey indicated that PDT-induced ER vacuole formation is not restricted to the photosensitizer Photofrin. Guo et al. [2003] reported that cytoplasmic vacuoles of unknown origin could be detected in MCF7 breast cancer cells after preincubation (24 h) with calphostin C, a photoactivatable drug and a PKC inhibitor, and exposing cells to fluorescent light (2 h). Subsequently, using DsRed-ER tracker as a tool, another report found that the cytoplasmic vacuoles elicited by calphostin C-mediated PDT in MCF7 cells were derived from the ER [Kaul and Maltese, 2009]. ER vacuolization triggered by calphostin C may be associated with a general increase in cellular ROS levels, leading to protein oxidation and/or carbonylation, in turn contributing to protein misfolding [Chiarini et al., 2008]. In acute lymphoblastic leukemia cells, calphostin C treatment was shown to induce rapid calcium mobilization from intracellular stores, an effect that appeared to be independent of PKC inhibition [Zhu et al., 1998]. In addition, calphostin C treatment interfered with vesicular protein export [Fabbri et al., 1994]. Because most of the findings of the present study are similar to the previously reported cellular effects of calphostin C photoexcitation, it seems likely that calcium imbalance and/or protein misfolding may play a role in the ER vacuolization induced by type II PDT treatment in A431 cells.

Results from some recent studies have provided important clues for understanding how ER vacuoles are generated in cells responding to external stimuli. It has been reported that accumulation of misfolded proteins in cells treated simultaneously with geldanamycin (an inhibitor of heat-shock protein 90) and bortezomib (a proteasome inhibitor which has been clinically approved to treat solid tumors) caused distention of the ER, a morphological alteration that was abolished by co-treating cells with cycloheximide to inhibit protein synthesis [Mimnaugh et al., 2006]. Heat-shock proteins are molecular chaperons that regulate protein folding and transport irreversibly damaged proteins to proteasomes for degradation. These observations indicate that concurrent blockage of cellular protein folding and degradation functions can cause severe ER stress and lead to ER membrane remodeling and vacuole formation. More recently, Szokalska et al. [2009] found that combined treatment with bortezomib and Photofrin-PDT caused ER vacuolization of tumor cells in vitro, and enhanced tumor cell killing and survival of mice in an immunogenic murine model. Interestingly, the cited authors found that neither Photofrin-PDT nor bortezomib alone caused significant ER vacuolization of tumor cells. These observations reinforce the importance of the proteasome-mediated protein degradation pathway in the etiology of ER vacuolization. In our present study, however, we found that extensive ER vacuolization could be triggered by type II Photofrin-PDT treatment alone, without the need for concurrent treatment with other drugs/stimuli. Between-study differences in Photofrin/laser doses and treatment paradigms may explain the divergent results; Szokalska et al. used a

24-h incubation with 10 μg/ml Photofrin and a total laser exposure (632.8 nm light) of 1.2 J/cm^2. In the present study, we incubated cells with 28 μg/ml Photofrin for 3 h and next without Photofrin for 21 h in fresh medium before exposure to a total laser dose of 5 J/cm^2 (632.8 nm light). Differences in cell lines (HeLa vs. A431) may also have contributed to variation in the results seen. Whether the type II Photofrin-PDT treatment used here is capable of inhibiting the activities of molecular chaperons and proteasomes remains an important question for future investigation. In addition, our observation that the ROS signal coincided well with the location of Photofrin, and occurred mainly around ER vacuoles (Fig. 3), suggests a possible role for direct and potent PDT-triggered oxidative damage of the lipids and proteins of the ER membrane in the ER vacuolization process, an intriguing possibility that deserves further study.

In conclusion, our present study unravels a route through which Photofrin-PDT treatment can induce extensive ER vacuolization (ER stress) of tumor cells in vitro. This ER stress, if not recovered, can cause cell death. Our findings identify an alternate death mechanism in the Photofrin-PDT-induced cell responses, and might provide a useful clue to clinicians to refine the Photofrin-PDT protocol for management of cancer in the future.

ACKNOWLEDGMENTS

We greatly appreciate Dr. Cheng-Jen Chang (Department of Plastic Surgery, Chang Gung Memorial Hospital, Taipei, Taiwan, Republic of China) for providing Photofrin.

REFERENCES

Agarwal ML, Clay ME, Harvey EJ, Evans HH, Antunez AR, Oleinick NL. 1991. Photodynamic therapy induces rapid cell death by apoptosis in L5178Y mouse lymphoma cells. Cancer Res 51:5993–5996.

Buettner GR, Kelley EE, Burns CP. 1993. Membrane lipid free radicals produced from L1210 murine leukemia cells by photofrin photosensitization: An electron paramagnetic resonance spin trapping study. Cancer Res 53:3670–3673.

Buytaert E, Callewaert G, Hendrickx N, Scorrano L, Hartmann D, Missiaen L, Vandenheede JR, Heirman I, Grooten J, Agostinis P. 2006. Role of endoplasmic reticulum depletion and multidomain proapoptotic BAX and BAK proteins in shaping cell death after hypericin-mediated photodynamic therapy. FASEB J 20:756–758.

Buytaert E, Dewaele M, Agostinis P. 2007. Molecular effectors of multiple cell death pathways initiated by photodynamic therapy. Biochim Biophys Acta 1776:86–107.

Castano AP, Mroz P, Hamblin MR. 2006. Photodynamic therapy and anti-tumour immunity. Nat Rev Cancer 6:535–545.

Chan WH, Yu JS, Yang SD. 2000. Apoptotic signalling cascade in photosensitized human epidermal carcinoma A431 cells: Involvement of singlet oxygen, c-Jun N-terminal kinase, caspase-3 and p21-activated kinase 2. Biochem J 351:221–232.

Chiarini A, Whitfield JF, Pacchiana R, Armato U, Dal Pra I. 2008. Photo-excited calphostin C selectively destroys nuclear lamin B1 in neoplastic human and rat cells—A novel mechanism of action of a photodynamic tumor therapy agent. Biochim Biophys Acta 1783:1642–1653.

Danial NN, Korsmeyer SJ. 2004. Cell death: Critical control points. Cell 116:205–219.

Dellinger M. 1996. Apoptosis or necrosis following Photofrin photosensitization: Influence of the incubation protocol. Photochem Photobiol 64:182–187.

Demaurex N, Distelhorst C. 2003. Cell biology. Apoptosis—The calcium connection. Science 300:65–67.

Denmeade SR, Isaacs JT. 2005. The SERCA pump as a therapeutic target: Making a ''smart bomb'' for prostate cancer. Cancer Biol Ther 4:14–22.

Dolmans DE, Fukumura D, Jain RK. 2003. Photodynamic therapy for cancer. Nat Rev Cancer 3:380–387.

Dougherty TJ, Gomer CJ, Henderson BW, Jori G, Kessel D, Korbelik M, Moan J, Peng Q. 1998. Photodynamic therapy. J Natl Cancer Inst 90:889–905.

Du Y, Ferro-Novick S, Novick P. 2004. Dynamics and inheritance of the endoplasmic reticulum. J Cell Sci 117:2871–2878.

Fabbri M, Bannykh S, Balch WE. 1994. Export of protein from the endoplasmic reticulum is regulated by a diacylglycerol/phorbol ester binding protein. J Biol Chem 269:26848–26857.

Gibson SL, Murant RS, Hilf R. 1988. Photosensitizing effects of hematoporphyrin derivative and photofrin II on the plasma membrane enzymes 5′-nucleotidase, Na^+ K^+-ATPase, and Mg^{2+}-ATPase in R3230AC mammary adenocarcinomas. Cancer Res 48:3360–3366.

Girotti A. 1990. Photosensitized lipid peroxidation in biological membranes. In: Kessel D editors. Photodynamic therapy of neoplastic disease. Florida: CRC. pp 229–245.

Gomer CJ, Razum NJ. 1984. Acute skin response in albino mice following porphyrin photosensitization under oxic and anoxic conditions. Photochem Photobiol 40:435–439.

Granville DJ, Ruehlmann DO, Choy JC, Cassidy BA, Hunt DW, van Breemen C, McManus BM. 2001. Bcl-2 increases emptying of endoplasmic reticulum Ca^{2+} stores during photodynamic therapy-induced apoptosis. Cell Calcium 30:343–350.

Guo B, Hembruff SL, Villeneuve DJ, Kirwan AF, Parissenti AM. 2003. Potent killing of paclitaxel- and doxorubicin-resistant breast cancer cells by calphostin C accompanied by cytoplasmic vacuolization. Breast Cancer Res Treat 82:125–141.

Halliwell B, Gutteridge JMC. 1989. Free radicals in biology and medicine. New York: Oxford University Press. p 936.

He XY, Sikes RA, Thomsen S, Chung LW, Jacques SL. 1994. Photodynamic therapy with photofrin II induces programmed cell death in carcinoma cell lines. Photochem Photobiol 59:468–473.

Henderson BW, Dougherty TJ. 1992. How does photodynamic therapy work? Photochem Photobiol 55:145–157.

Hsieh YJ, Wu CC, Chang CJ, Yu JS. 2003. Subcellular localization of Photofrin determines the death phenotype of human epidermoid carcinoma A431 cells triggered by photodynamic therapy: When plasma membranes are the main targets. J Cell Physiol 194:363–375.

Hsu RM, Tsai MH, Hsieh YJ, Lyu PC, Yu JS. 2010. Identification of MYO18A as a novel interacting partner of the PAK2/betaPIX/GIT1 complex and its potential function in modulating epithelial cell migration. Mol Biol Cell 21:287–301.

Kaul A, Maltese WA. 2009. Killing of cancer cells by the photoactivatable protein kinase C inhibitor, calphostin C, involves induction of endoplasmic reticulum stress. Neoplasia 11:823–834.

Kessel D, Luo Y. 1998. Mitochondrial photodamage and PDT-induced apoptosis. J Photochem Photobiol B 42:89–95.

Kessel D, Luo Y, Deng Y, Chang CK. 1997. The role of subcellular localization in initiation of apoptosis by photodynamic therapy. Photochem Photobiol 65:422–426.

Kessel D, Vicente MG, Reiners JJ, Jr. 2006. Initiation of apoptosis and autophagy by photodynamic therapy. Autophagy 2:289–290.

LeBel CP, Ischiropoulos H, Bondy SC. 1992. Evaluation of the probe 2′,7′-dichlorofluorescin as an indicator of reactive oxygen species formation and oxidative stress. Chem Res Toxicol 5:227–231.

Luo Y, Kessel D. 1997. Initiation of apoptosis versus necrosis by photodynamic therapy with chloroaluminum phthalocyanine. Photochem Photobiol 66:479–483.

Marchal S, Fadloun A, Maugain E, D'Hallewin MA, Guillemin F, Bezdetnaya L. 2005. Necrotic and apoptotic features of cell death in response to Foscan photosensitization of HT29 monolayer and multicell spheroids. Biochem Pharmacol 69:1167–1176.

Mimnaugh EG, Xu W, Vos M, Yuan X, Neckers L. 2006. Endoplasmic reticulum vacuolization and valosin-containing protein relocalization result from simultaneous hsp90 inhibition by geldanamycin and proteasome inhibition by velcade. Mol Cancer Res 4:667–681.

Moan J, Berg K. 1991. The photodegradation of porphyrins in cells can be used to estimate the lifetime of singlet oxygen. Photochem Photobiol 53:549–553.

Murant RS, Gibson SL, Hilf R. 1987. Photosensitizing effects of Photofrin II on the site-selected mitochondrial enzymes adenylate kinase and monoamine oxidase. Cancer Res 47:4323–4328.

Noodt BB, Berg K, Stokke T, Peng Q, Nesland JM. 1996. Apoptosis and necrosis induced with light and 5-aminolaevulinic acid-derived protoporphyrin IX. Br J Cancer 74:22–29.

Noodt BB, Berg K, Stokke T, Peng Q, Nesland JM. 1999. Different apoptotic pathways are induced from various intracellular sites by tetraphenylporphyrins and light. Br J Cancer 79:72–81.

Oleinick NL, Morris RL, Belichenko I. 2002. The role of apoptosis in response to photodynamic therapy: What, where, why, and how. Photochem Photobiol Sci 1:1–21.

Orrenius S, Zhivotovsky B, Nicotera P. 2003. Regulation of cell death: The calcium-apoptosis link. Nat Rev Mol Cell Biol 4:552–565.

Peng Q, Moan J, Nesland JM. 1996. Correlation of subcellular and intratumoral photosensitizer localization with ultrastructural features after photodynamic therapy. Ultrastruct Pathol 20:109–129.

Roberts WG, Liaw LH, Berns MW. 1989. In vitro photosensitization II. An electron microscopy study of cellular destruction with mono-L-aspartyl chlorin e6 and photofrin II. Lasers Surg Med 9:102–108.

Sakharov DV, Elstak ED, Chernyak B, Wirtz KW. 2005. Prolonged lipid oxidation after photodynamic treatment. Study with oxidation-sensitive probe C11-BODIPY581/591. FEBS Lett 579:1255–1260.

Salet C. 1986. Hematoporphyrin and hematoporphyrin-derivative photosensitization of mitochondria. Biochimie 68:865–868.

Szokalska A, Makowski M, Nowis D, Wilczyński GM, Kujawa M, Wójcik C, Młynarczuk-Biały I, Salwa P, Bil J, Janowska S, Agostinis P, Verfaillie T, Bugajski M, Gietka J, Issat T, Głodkowska E, Mrówka P, Stoklosa T, Hamblin MR, Mróz P, Jakóbisiak M, Golab J. 2009. Proteasome inhibition potentiates antitumor effects of photodynamic therapy in mice through induction of endoplasmic reticulum stress and unfolded protein response. Cancer Res 69:4235–4243.

Thomas JP, Girotti AW. 1989. Role of lipid peroxidation in hematoporphyrin derivative-sensitized photokilling of tumor cells: Protective effects of glutathione peroxidase. Cancer Res 49:1682–1686.

Vedrenne C, Hauri HP. 2006. Morphogenesis of the endoplasmic reticulum: Beyond active membrane expansion. Traffic 7:639–646.

Woods JA, Traynor NJ, Brancaleon L, Moseley H. 2004. The effect of photofrin on DNA strand breaks and base oxidation in HaCaT keratinocytes: A comet assay study. Photochem Photobiol 79:105–113.

Wu CC, Chien KY, Tsang NM, Chang KP, Hao SP, Tsao CH, Chang YS, Yu JS. 2005. Cancer cell-secreted proteomes as a basis for searching potential tumor markers: Nasopharyngeal carcinoma as a model. Proteomics 5:3173–3182.

Zhu DM, Narla RK, Fang WH, Chia NC, Uckun FM. 1998. Calphostin C triggers calcium-dependent apoptosis in human acute lymphoblastic leukemia cells. Clin Cancer Res 4:2967–2976.